Available online at www.sciencedirect.com
SCIENCE DIRECT®
Journal of Molecular Catalysis A: Chemical 227 (2005) 223–229
JOURNAL OF MOLECULAR CATALYSIS A: CHEMICAL
www.elsevier.com/locate/molcata

Theoretical study of catalytic steam cracking on a asphaltene model molecule

Iván Machín[a,*], Juan Carlos de Jesús[a], Guaicaipuro Rivas[a], Ingrid Higuerey[a], José Córdova[a], Pedro Pereira[a], Fernando Ruette[b], Aníbal Sierraalta[b]

[a] *INTEVEP, Edo. Miranda, P.O. Box 76343, Caracas 1070-A, Venezuela*
[b] *IVIC, Lab. de Química Computacional, Apdo. 21827, Caracas 1020-A, Venezuela*

Received 6 February 2004; accepted 26 April 2004
Available online 8 December 2004

Abstract

In the present work, a quantum mechanics parametric method was employed to evaluate the interaction of metallic nickel, potassium, and water with an asphaltene model molecule (AMM). A reaction scheme is proposed for a catalytic steam cracking (CSC) process based on the formation and breaking of bonds. It was found a very important interaction between metallic nickel with nitrogen, and sulfur atoms of the asphaltene molecule, which leads to the formation of nickel–asphaltene intermediate complexes. Also, it was observed that nickel–asphaltene complexes are able to dissociate water and in such cases asphaltene molecules may be hydrogenated. Electron transfer from potassium to asphaltene systems promotes the H_2O dissociation on Ni and favors C–S and C–N bond activations.

Keywords: Steam cracking; Nickel catalyst; Asphaltene; Parametric method

1. Introduction

Interaction of water with carbon compounds (water + feed) involves several processes: (a) steam reforming, (b) water gas shift (WGS), (c) coal gasification, and (d) steam cracking. Processes (a–c) comprise the formation of CO, CO_2, and H_2 with the presence of a catalyst [1–4].

The steam cracking process can be carried out, in two possible fashions, with and without a catalyst. The former entails a reaction of water with hydrocarbons (naphtha) at high temperatures (600–750 °C) to produce CO, CO_2, and H_2, avoiding coke generation. On the other hand, the catalytic steam cracking (CSC) [5–8] is a conversion of heavy crude and residuals at lower temperatures (400–430 °C) in the presence of water, alkali and transition metal compounds [7,8]. A bifunctional mechanism for CSC process was proposed by Pereira and coworkers [6]:

$$H_2O \xrightarrow{\text{Catalyst A}} 2H^\circ + O^\circ \quad (2)$$

The CSC process also generates CO and CO_2, but in small quantities.

As far as we know, a modeling on this type of systems has not been performed yet. In this work, quantum mechanical calculations were carried out in order to model the CSC process for heavy oil. New insights of the CSC mechanism are proposed based on the qualitative results of these calculations. This publication is organized in the following way. (a) A brief description of the theoretical method and the feasibility of using a very simple model for the CSC reaction are presented in the next section. (b) Discussion of results is shown in Section 3, by analyzing calculated properties of different systems (asphaltene fragment, asphaltene–metal, asphaltene–metal–H_2O, each of them with charges 0 and −1). (c) Finally, a resume of the most remarkable results and some recommendations for future works are exposed in Section 4.

* Corresponding author.
E-mail address: machini@pdvsa.com (I. Machín).

1381-1169/$ – see front matter © 2004 Elsevier B.V. All rights reserved.
doi:10.1016/j.molcata.2004.04.048

2. Theoretical method and reaction model

A quantum chemistry (QC) parametric method (CATIVIC program [9,10]) was employed in this work. This method is based on simulation techniques, using parametric functionals to mimic the total energy functional [11,12]. The molecular parameters α_{XY} and β_{XY} are calculated for X–Y, S–N, and S–O diatomic molecules (X = Ni; Y = H, C, N, O, S), using an iterative procedure and a diatomic molecular data base [10]. Other parameters were obtained from MINDO/SR method [13] that is an extension of MINDO/3 [14] for transition metals. MINDO/SR method reproduces very well Ni–C and Ni–H interactions [15] as well as surface reactions on metallic clusters that have been improved in CATIVIC. Molecular parameters used in this study are shown in Table 1.

CATIVIC program evaluates diatomic energy (DE), diatomic binding energy (DBE), Mulliken charges, and interatomic distances. DBE values are a manifestation of the bond strength obtained by means of the following equation [16]:

$$\mathrm{DBE(X{-}Y)} = \mathrm{DE_{XY}} + f_{\mathrm{Y}}(\mathrm{X{-}Y})\varepsilon_{\mathrm{X}} + f_{\mathrm{X}}(\mathrm{X{-}Y})\varepsilon_{\mathrm{Y}} \quad (4)$$

$$f_{\mathrm{X}}(\mathrm{X{-}Y}) = \frac{\mathrm{DE_{XY}}}{\sum_{\mathrm{X>C}} \mathrm{DE_{XC}}} \quad (5)$$

where ε_{X} and $\mathrm{DE_{XY}}$ are monoatomic and diatomic energies for atom X and X–Y bond, respectively [17].

Simple models were selected to simulate the CSC reaction components; i.e, fragments of asphaltene molecule that represent the heavy crude oil; a nickel atom to mimic the transition metal catalyst; a water molecule to simulate the steam; and a negative charge to emulate the presence of an alkali metal.

The selected asphaltene model molecule (AMM) is average molecule that reproduces a set of physical–chemical properties of the Tia Juana Venezuelan heavy crude oil 500 + residue, as shown in Reference [18]. The AMM was divided into several fragments, based on the heteroatom location. F1 and F2 fragments (see Fig. 1) were selected because they are the most common found in different asphaltene molecular frames. In addition, they have importance

Table 1
Molecular parameters used in CATIVIC method

Molecular parameter atom pair	β	α	Reference
Ni–C	0.6296	1.0833	Present work
Ni–N	0.7876	1.3037	Present work
Ni–O	1.3087	2.1595	Present work
Ni–S	0.7871	3.1545	Present work
S–C	0.2846	0.9320	[14]
C–C	0.4199	0.7255	[14]
C–N	0.4108	0.8653	[14]
C–H	0.3150	0.7809	[14]
S–S	0.2024	0.9269	[14]
S–H	0.2206	0.8999	[14]
S–N	0.3019	1.0502	Present work
S–O	0.4450	0.9840	Present work

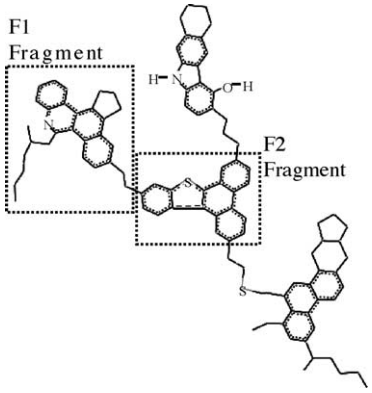

Fig. 1. Asphaltene model molecule (AMM).

in hidrodesulfurization (HDS) and hydrodenitrogenation (HDN) processes of heavy oil.

It is familiar that alkaline metals in the gasification of carbon improve the efficiency of this process. It follows the order: Cs > K > Na > Li [4]. The order is explained considering that the Cs has greater capacity of giving electrons than the potassium, and so on. The promoting effect of K may be associated with an increasing in the electronic density on the aromatic hydrocarbon, due to the electronic transfer from the metal to the carbon compound. In order to simulate the presence of an alkali compound (potassium compound) on aromatic hydrocarbons, a negatively charged system was selected, as it has been also done in a previous work [19]. The interaction of potassium compounds with aromatic compounds (R) has been reported experimentally by Stevenson et al. [20]. They show the formation of anion radical salts ($\mathrm{R^-\cdots K^+}$). In addition, experimental results of potassium salts on graphite surface confirm electronic density transfer from the metal to the aromatic system [21], as has been theoretically substantiated by Natori et al. [22].

The presence of $\mathrm{K^\circ}$ is supported by experimental findings of Kotarba et al. [23]. They report that a thermal desorption of potassium atoms from KOH can occur on transition metal carbides and nitrides. On the other hand, calculation of Gibb's free energy at 427 °C, carried out with the thermodynamic software, THERMO4 [24], for the following reaction:

$$\begin{aligned} &3\mathrm{K_2O} + \mathrm{C_7H_8(g)} \\ &\quad \rightarrow 4\mathrm{K^\circ} + \mathrm{K_2CO_3} + \mathrm{C_6H_6(g)} + \mathrm{H_2(g)}, \\ &\quad \Delta G = -42\,\mathrm{kcal/mol}, \end{aligned} \quad (6)$$

shows that $\mathrm{K^\circ}$ can be available in a hydrocarbon mixture, such as a heavy crude oil. Finally, the $\mathrm{Ni^\circ}$ presence is reported by experimental findings of metallic nickel nanoparticles synthesis in water-in-oil [25].

Thus, these experimental results justify the reaction model of $\mathrm{K^\circ}$ atoms that interact on asphaltene molecule and after that the system interrelates with metallic nickel in the presence of $\mathrm{H_2O}$.

3. Results and discussion

The asphaltene molecule (Fig. 1) was full optimized using the QC program. From this final geometry, neutral fragments F1 and F2 were selected. Then, Ni interactions with F1 and F2 fragments were carried out by optimizing F*I*–Ni (*I* = 1, 2) systems, starting at different *s* sites, directly located above N, S, and C_i (for example, *i* = 1–6) atoms at different Ni–*s* distances, (scanning from 3.0 to 1.5 Å), see Figs. 2–3.

Results of the interaction Ni with F1 fragment (see Fig. 2) show that Ni adsorption directly on C atoms is not possible because interactions are repulsive. Nevertheless, starting at 1.82 Å in the region around the N atom, the formation of a stable complex [F1–Ni]° occurs.

DBE values and equilibrium bond distance (EBD) for selected bonds of F1 and [F1–Ni]° are displayed in Table 2. The complex stability may be explained by the making of Ni–C_1 and Ni–N bonds with DBE values of −18 and −12 kcal/mol, respectively. However, the formation this complex is endothermic (about 38 kcal/mol less stable than the sum of separated systems (Ni + F1)); therefore, [F1–Ni]° may be considered as a metastable reaction intermediate. The feasibility of this intermediate is supported by the existence of

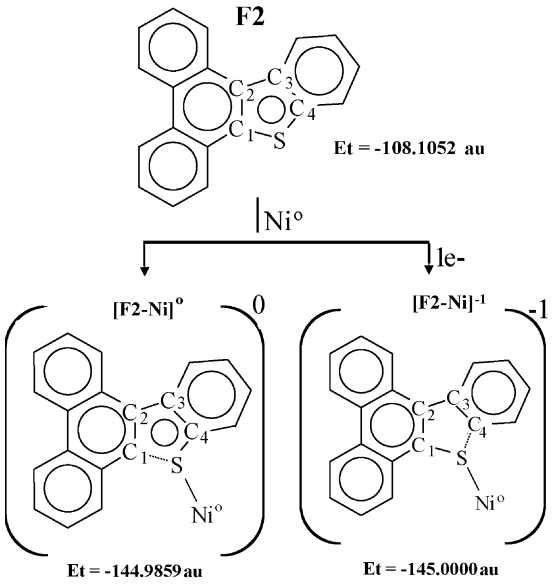

Fig. 3. Scheme of Ni interactions with fragment F2 of AMM.

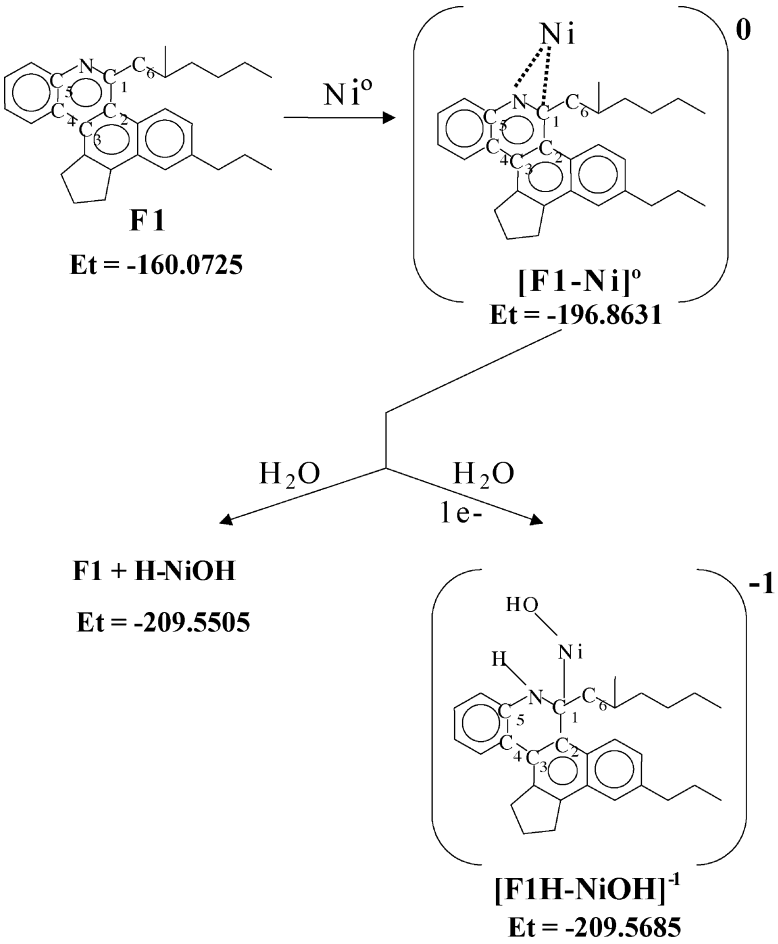

Fig. 2. Scheme of Ni and water interactions with fragment F1 of AMM.

Table 2
Diatomic bond energies (DBE) (kcal/mol) and equilibrium bond distances (EBD) ((Å), values in parentheses) for F1, [F1–Ni]°, and $[F1–NiH_2O]^{-1}$ systems (see Fig. 2)

System bond	F1	[F1–Ni]°	$[F1]^{-1}$	$[F1–NiH_2O]^{-1}$
N–C_1	−127 (1.368)	−77 (1.438)	−123 (1.340)	−78 (1.455)
C_1–C_2	−113 (1.498)	−97 (1.540)	−125 (1.439)	−100 (1.552)
C_2–C_3	−105 (1.445)	−124 (1.464)	−112 (1.487)	−98 (1.546)
C_3–C_4	−106 (1.485)	−104 (1.517)	−109 (1.485)	−120 (1.458)
C_4–C_5	−122 (1.451)	−120 (1.457)	−119 (1.465)	−117 (1.457)
C_5–N	−103 (1.368)	−88 (1.400)	−114 (1.360)	−104 (1.352)
C_6–C_1	−98 (1.519)	−82 (1.584)	−97 (1.514)	−81 (1.608)
C_1–Ni	–	−18 (2.027)	–	−54 (2.061)
N–Ni	–	−12 (1.797)	–	−0 (2.564)
Ni–O	–	–	–	−118 (1.749)
N–H	–	–	–	−75 (1.003)

Ni–pyridine complexes, as has been reported in the literature [26–27].

It is also clear from Table 2 that noticeable weakenings of 50, 15, and 16 kcal/mol occur in N–C_1, N–C_5, and C_1–C_2 bonds, respectively. These results are in correlation with the elongation of the corresponding C–N and C–C bonds in [F1–Ni]° with respect to F1, see EBD values in parentheses. Thus, DBE and EBD results indicate an important activation of the N–C_1 bond. There is also an enlargement and shortening of other EBDs in the rest of C–C bonds in the asphaltenic system. This effect is due to the lost of aromaticity, owing to the formation of Ni–C_1 and Ni–N bonds.

Table 3 shows atomic charges on selected atoms. It is clear that there is a net transfer of 0.39 electrons from the metal to hydrocarbon atoms, especially to C_1 atom. However, this transferred charge is not totally localized on interacting atoms, but it is spread over the whole structure.

Results of the interaction of H_2O with [F1–Ni]° complex show that adsorption of water on the Ni atom occurs with a breaking of the [F1–Ni]° bond (see Fig. 2). The formation of a strong Ni–O (DBE(Ni–O) = −119 kcal/mol) and Ni–H (DBE(Ni–H) = −75 kcal/mol) bonds leads to the H–Ni–OH compound. These results are expected because dissociation of water on Ni has been reported as well as in experimental and theoretical studies [28–30].

Results of total energy (E_t = −160.1072) for $[F1]^{-1}$ radical show that is more stable than $[F1]^0$ (E_t = −160.0725) with a difference of about 22 kcal/mol. This result is supported by electron affinity experimental values of aromatic hydrocarbons with heteroatomic substituents [31]. Bond strength (DBE values) analysis in Table 2 indicates that most of the bonds in $[F1]^{-1}$ are strengthened, as compared with $[F1]^0$.

Table 3
Charges on selected atoms for F1, [F1–Ni]°, $[F1–NiH_2O]°$, and $[F1–NiH_2O]^{-1}$ systems (see Fig. 2)

System Atom	F1	[F1–Ni]°	$[F1–NiH_2O]^{-1}$	H_2O
N	−0.14	−0.01	−0.07	–
C_1	−0.00	−0.11	−0.01	–
C_2	−0.06	−0.03	−0.11	–
C_3	0.00	0.01	−0.02	–
C_4	−0.01	−0.02	−0.03	–
C_5	0.10	0.04	0.08	–
C_6	0.06	0.02	−0.02	–
Ni	–	0.39	−0.04	–
H	–	–	0.07	0.25
O	–	–	−0.32	−0.50

Calculations of Ni° interaction with $[F1]^{-1}$ show that the formation of a charged $[F1–Ni]^{-1}$ complex it is not possible. The F1 · · · Ni interaction is repulsive for all F1 sites on the negatively charged system. Nevertheless, calculations reveal that if Ni and H_2O molecule are approached close to nitrogen atom of F1, water is dissociated and a $[F1H–NiOH]^{-1}$ complex is formed (see Fig. 2). DBEs values in Table 2 show several features: the formation of a strong Ni–OH bond (−118 kcal/mol); an N–H bond (−75 kcal/mol); the scission of the Ni–N bond; and the formation of a C_1–Ni bond (−54 kcal/mol) that is stronger than that in [F1–Ni]° (−18 kcal/mol). These results may help to understand a role of K in the CSC process. Potassium makes easy the dissociation of H_2O on Ni site and facilitates a hydrogen transfer from the water molecule to the organic fragment. Note that the resultant organic product (F1H), after decomposition of $[F1H–NiOH]^{-1}$, will have an upgraded quality, because it has been hydrogenated. Formation of NiOH due to H_2O interaction on Ni surfaces has been reported by Zaera and coworkers [32] at low temperatures. Notice also that the Ni–C_1 bond is relatively weak (−54 kcal/mol) and can be cleaved by the assistance of another H_2O molecule, leading to the formation of $Ni(OH)_2$. It is well-known that $Ni(OH)_2$ is formed in aqueous solutions of Ni(II) salts with addition of alkali-metal hydroxides [33].

In order to study the interaction of the Ni atom with the sulphurized part of the asphaltene molecule, calculations were carried out for the interaction of the fragment F2 and a Ni° atom (see Fig. 3). As in F1 case, the interaction is favored on the heteroatom of the F2 fragment, leading to the formation of a [F2–Ni]° complex. Nevertheless, the interaction is stronger than in the [F1–Ni]° complex. Thus, DBE values given in Table 4 indicate the formation of a Ni–S bond (−83 kcal/mol) and the weakening of S–C_1 and S–C_4 bonds (from −100 to −26 and from −102 to −81 kcal/mol, respectively). In addition, a change in the S–C_1 bond distance (from

Table 4
Diatomic bond energies (kcal/mol) and equilibrium bond distances ((Å), values in parentheses) for F2, [F2–Ni]°, $[F2–Ni]^{-1}$, [F2–NiH_2O]°, and $[F2–NiH_2O]^{-1}$ systems (see Figs. 3–5)

System bond	F2	[F2–Ni]°	$[F2–Ni]^{-1}$	[F2–NiH_2O]° (A°)	[F2–NiH_2O]° (B°)	$[F2–NiH_2O]^{-1}$ (A^-)	$[F2–NiH_2O]^{-1}$ (B^-)
S–C_1	−100 (1.753)	−26 (2.073)	−76 (1.816)	−25 (2.141)	0 (3.487)	−81 (1.799)	−48 (1.884)
C_1–C_2	−129 (1.389)	−100 (1.498)	−106 (1.511)	−99 (1.516)	−132 (1.418)	−115 (1.447)	−131 (1.421)
C_2–C_3	−110 (1.486)	−124 (1.438)	−125 (1.429)	−122 (1.460)	−110 (1.512)	−118 (1.468)	−110 (1.498)
C_3–C_4	−115 (1.439)	−110 (1.448)	−120 (1.449)	−111 (1.456)	−120 (1.428)	−121 (1.439)	−122 (1.443)
S–C_4	−102 (1.750)	−81 (1.785)	−20 (2.179)	−87 (1.762)	−69 (1.721)	−22 (2.178)	−2 (2.810)
S–Ni	–	−83 (2.010)	−97 (1.987)	−123 (2.032)	−68 (2.194)	−125 (1.994)	−91 (2.178)
Ni–OH	–	–	–	−79 (1.941)	−144 (1.745)	−69 (1.953)	−133 (1.744)
C_1–H_a	–	–	–	–	−93 (1.109)	–	–
C_4–H_b	–	–	–	–	–	–	−85 (1.120)

Table 5
Charges on selected atoms of F2, [F2–Ni]°, $[F2–Ni]^{-1}$, [F2–NiH_2O]°, and $[F2–NiH_2O]^{-1}$ systems (see Figs. 3–5)

System atom	H_2O	F2	[F2–Ni]°	$[F2–Ni]^{-1}$	[F2–NiH_2O]° (A°)	[F2–NiH_2O]° (B°)	$[F2–NiH_2O]^{-1}$ (A^-)	$[F2–NiH_2O]^{-1}$ (B^-)
S	–	−0.22	−0.74	−0.78	−0.76	−0.40	−0.79	−0.74
C_1	–	0.14	−0.06	0.08	−0.05	−0.04	0.09	−0.05
C_2	–	−0.05	0.01	−0.18	0.01	0.01	−0.16	−0.03
C_3	–	−0.02	−0.00	0.10	−0.01	0.02	0.08	0.05
C_4	–	0.14	0.16	−0.06	0.15	0.09	−0.04	−0.03
Ni	–	–	0.69	0.58	0.38	0.25	0.30	0.21
H_a	0.25	–	–	–	0.32	0.04	0.29	0.18
H_b	0.25	–	–	–	0.32	0.22	0.30	0.11
O	−0.50	–	–	–	−0.19	−0.29	−0.18	−0.30

1.753 to 2.037 Å) reveals that the Ni atom strongly activates this bond.

Table 5 shows a higher electronic charge transfer from the Ni atom to the organic fragment (0.69 electrons) in [F2–Ni]° than in [F1-Ni]° (0.39 e^-). This charge is mainly located on the S atom.

Interaction of Ni with the negatively charged fragment leads to a stable $[F2–Ni]^{-1}$ complex with a strong bond Ni–S of −97 kcal/mol, see Fig. 3 and Table 4. As in the neutral complex, there is a weakening and an enlargement of S–C bonds: S–C_1 (DBEs vary from −100 to −76 kcal/mol and EBDs change from 1.753 to 1.816 Å) and S–C_4 (from −102 to −20 kcal/mol and from 1.750 to 2.179 Å), see also Table 4. It is also evident that in the negative complex the S–C_4 bond is more activated than the S–C_1 one. The very high activation of the S–C_4 bond can be explained by the formation of a Ni–S bond and the antibonding nature of LUMO (centered on the S–C_4 bond) in F2. Results of Table 5 indicate that there is a net electronic charge transfer from the Ni atom (0.58 electrons) to the organic fragment, primarily to S and C_4 atoms. According to above results, the S–C_1 bond in [F2–Ni]° is somewhat destabilized, while in $[F2–Ni]^{-1}$ the S–C_4 bond is deeply weakened. Therefore, the electronic transfer form K atom seems to determine the place in which the S–C activation occurs.

The study of H_2O interaction with [F2–Ni]° reveals that two intermediate complexes (A° and B°, see Table 4 and Fig. 4) can be formed, depending on the approaching manner of H_2O to S–C bonds. There is a complete S–C_1 bond cleavage in the B° complex, while in the A° the S–C_1 bond is weakened to −25 kcal/mol. In complex B°, the Ni–water interaction leads to H_2O dissociation with S–C_4, S–Ni, and Ni–O bonds of −69, −68, and −144 kcal/mol, respectively. On the other hand, in A° the correspondent bonds are −87, −123, and −79 kcal/mol, respectively. The Ni–O bond is

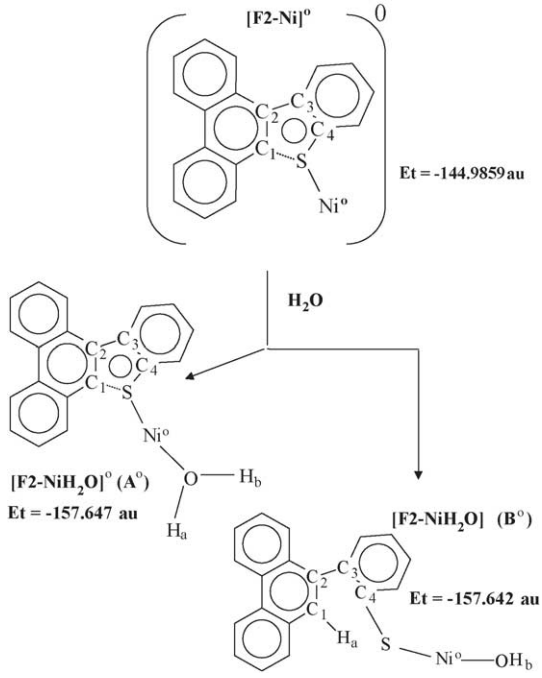

Fig. 4. Scheme of the [F2–Ni]° intermediate interacting with H_2O.

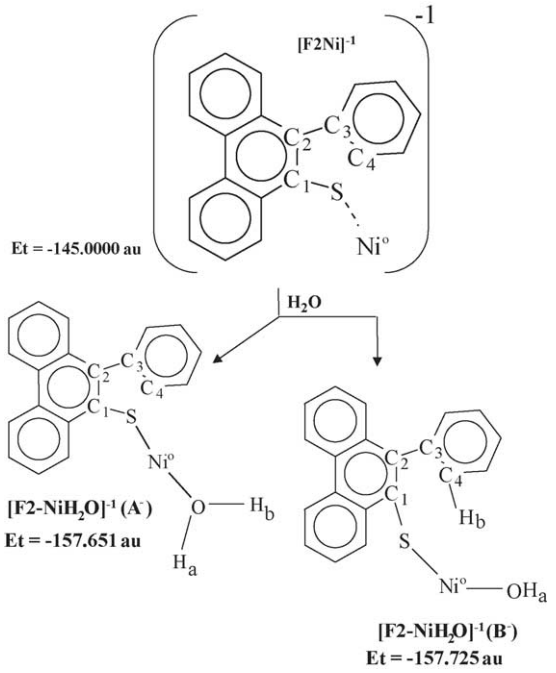

Fig. 5. Scheme of the $[F2–Ni]^{-1}$ intermediate interacting with H_2O.

weaker in A° complex than in B° one, because in the former O shares its electrons with three bonds (Ni–O, O–H_a, and O–H_b) and in the later the H_a atom is forming a C_1–H_a bond of −93 kcal/mol. Results also suggest that the B° complex could be an intermediate in a sulfur removal reaction because of S–C1 breaking, formation of C_1–H_a, and S–C_4 bond activation (from −102 to −69 kcal/mol), which may undergo thermal cleavage.

The charge analysis (see Table 5) indicates that there is an electronic charge transfer from the Ni atom to the organic fragment in both complexes. This transfer is lower in magnitude than in the case of complex without H_2O. It is observed also a withdrawing of electronic charge from the H_2O molecule to [F2–Ni]° in the A° complex. This is probably due to the large positive charge of 0.69 au on Ni in [F2–Ni]°.

Results for the interaction of $[F2–Ni]^{-1}$ complex with a water molecule show, as in the case of the neutral complex, that exist two complexes $[F2–NiH_2O]^{-1}$ (A^- and B^-, see Fig. 5) hinging on the H_2O approaching way to the S–C bonds. The total energies (E_t) comparison between neutral and charged complexes (see Figs. 5 and 4) seems to indicate that a role of K is also to stabilize the formed complexes. Particularly, B^- (E_t = −157.725 au) is more stable than B° (E_t = −157.642 au); therefore, it promotes sulfur removal reaction in F2-type fragments. In addition, the sum of SC_1 and S–C_4 bond strengths (−112 and −69 kcal/mol for A° and B°, respectively) in neutral intermediates indicate that are less activated than in the charged ones (−103 and −50 kcal/mol for A^- and B^-, respectively). The S–C_4 is almost broken (−2 kcal/mol) and the S–C_1 is fairly activated (from −100 in F2 to −48 kcal/mol in B^-), suggesting that B^- complex is almost ready to remove S atom from asphaltene.

An analysis of all results mentioned above let us to propose new mechanistic features in the CSC process by considering four elementary steps: (a) interaction of the asphaltene (R–X) with the metallic nickel (Ni°) yields a complex ([R–X–Ni]°) in which bonding interactions are mainly completed by means of heteroatoms (X = N, S). (b) Formation of a negatively charged complex ($[R–X–Ni^\circ]^{-1}$ K^+) occurs if the X–Ni in the neutral complex is relatively strong, for example in [F2–Ni]°. (c) Water adsorption on a metallic site (Ni°) of $[R–X–Ni^\circ]^{-1}$ complex gives $[R–X–NiOH_2]^{-1}$. (d) Finally, hydrogenation of asphaltene fragment R–X occurs by water dissociation $[HR–X–NiOH]^{-1}$. This mechanism could be schematized as follows:

$$R–X + Ni^\circ \rightarrow [R–X–Ni]^\circ \quad (7)$$

$$[R–X–Ni]^\circ + K^\circ \rightarrow [R–X–Ni]^{-1}K^{+1} \quad (8)$$

$$H_2O + [R–X–Ni]^{-1}K^{+1} \rightarrow [R–X–Ni\cdots OH_2]^{-1}K^{+1} \quad (9)$$

$$[R–X–Ni\cdots OH_2]^{-1}K^{+1} \rightarrow [HR–X–Ni–OH]^{-1}K^{+1}. \quad (10)$$

The $[HR–X–Ni–OH]^{-1}$ K^{+1} complex can interact with another H_2O molecule to yield a hydrogenated asphaltene molecule and $Ni(OH)_2$, as mentioned above. However, in some cases this interaction may remove the X heteroatom, giving $H_2R + X–Ni(OH)_2$, for example, S–$Ni(OH)_2$ in the F2 fragment, because the S–C_1 bond is fairly activated. Thus, these results predict also the possibility of a HDS during the CSC process.

4. Concluding remarks and comments

Modeling of catalytic steam cracking reaction using asphaltene fragments and a Ni atom as a catalyst can give results that may be used to explain the upgrading of heavy and extraheavy crude oil quality. The most relevant issues can be enumerated as follows:

1. The interaction of a Ni° atom with the organic fragments F1 and F2 produces a bond between Ni° and asphaltenic heteroatoms (nitrogen and sulfur atoms). In each case, complex organometallic intermediates ([F1–Ni]° and [F2–Ni]°) are formed, with a charge transfer from the Ni atom to the organic fragments. This interaction turns out in a significant weakening of C–N and C–S bonds of aromatic systems, suggesting a later remotion of N and S atoms.
2. Potassium salts produces the $[F1]^{-1}$ and $[F2]^{-1}$ fragments and $[F2–Ni]^{-1}$ complex that are more stable than the correspondent neutral systems. The interaction of water, Ni, and asphaltene fragment (FI) yields a strong Ni–O bond

(FI–Ni–OH_2) and in some cases leads to water dissociation.

3. It was found hydrogen transference from the dissociated H_2O on Ni atom to the asphaltene, as well as in charged and neutral systems. In both cases, the interaction yields NiOH and a hydrogenated aromatic ring. In the case of F1, the hydrogen transfer takes place toward its N atom, only in the charged system; while in F2 fragment, it occurs toward one of the C atoms close to S on both [F2–Ni]$^{\circ}$ and [F2–Ni]$^{-1}$ intermediates.
4. The interaction of water with the neutral and charged intermediates ([F2–Ni]$^{\circ}$ and [F2–Ni]$^{-1}$) produces the scission of one of the S–C bonds. The electron transfer from potassium to the asphaltene fragment seems to control which S–C bond may be broken.
5. Results presented here suggest that the previous mechanism proposed by Pereira and coworkers [6] for asphaltene thermal cleavages can be complemented with the catalytic assistance of Ni–asphaltene interaction, K promotion, and H_2O dissociation.
6. A more complex model must be considered in future works. It should incorporate small Ni or NiO clusters and more than one H_2O molecule. In addition, an explicit representation of K compounds must be contemplated, in order to give a more realistic representation of the catalytic system. Comparison with others transition metals are now in progress.

Acknowledgment

This research has been supported by FONACIT under contract G-9700667.

References

[1] D.C. Grenouble, J. Catal. 75 (1982) 51.
[2] D. Duprez, J. Catal. 90 (1984) 292.
[3] G. Eartl, H. Knozinger, J. Weitkamp (Eds.), Handbook of Heterogeneous Catalysis, vol. 4, 1834, VCH Verlagsgesellschaft GmbH, Weinheinm, Federal Republic of Germany, 1997.
[4] P.J. Cassidy, W. Jackson, F.P. Larkins, M.P. Louey, R.J. Sakurovs, Fuel Process. Technol. 14 (1986) 231.
[5] P. Pereira, I. Machín, G. Salerno, E. Cotte, I. Higuerey, A. Andriollo, J. Córdoba, l. Zacarías, R. Marzín, G. Rivas, Acta Cient. Ven. 50 (1999) 48.
[6] J. Carrazza, P. Pereira, N. Martinez, United States Patent, Patent Number 5,688,395 (1997).
[7] P. Pereira, R. Marzín, L. Zacarías, J. Córdova, J. Carrazza, M. Mariño, United States Patent, Patent Number 5,885,441 (1999).
[8] P. Pereira, R. Marzín, L. Zacarías, I.L. Trosell, F. Hernández, J. Córdova, J. Szeoke, C. Flores, J. Duque, R.B. Solari, Visión Tecnológica 6 (1998) 5.
[9] F. Ruette, M. Sánchez, G. Martorell, R. Añez, L. Rodríguez, R. Martínez, A. Sierraalta, L. Rincón, C. Mendoza, Actas del XVIII Simposio Iberoamericano de Catálisis (2002) 112.
[10] (a) F. Ruette, M. Sánchez, G. Martorell, C. González, R. Añez, A. Sierraalta, L. Rincón, C. Mendoza, Int. J. Quantum Chem. 96 (2004) 321;
(b) F. Ruette, M. Sánchez, C. Mendoza, A. Sierraalta, G. Martorell, C. González, Int. J. Quantum Chem. 96 (2004) 303;
(c) R. Martínez, F. Brito, M.L. Araujo, F. Ruette, A. Sierraalta, Int. J. Quantum Chem. 97 (2004) 854.
[11] J.R. Primera, M. Romero, M. Sánchez, A. Sierralta, F. Ruette, J. Mol. Struct. (Theochem.) 469 (1999) 177.
[12] M. Romero, M. Sánchez, A. Sierraalta, L. Rincón, F. Ruette, J. Chem. Inform. Comp. Sci. 39 (1999) 543.
[13] G. Blyholder, J. Head, F. Ruette, Theor. Chim. Acta 60 (1982) 429.
[14] R.C. Bingham, M.J.S. Dewar, D.H. Lo, J. Am. Chem. Soc. 97 (1975) 1285.
[15] (a) F. Ruette, F.M. Poveda, in: E. Illisca, K. Makoshi (Eds.), Electron Processes at Solid Surfaces, World Scientific Publishing Co, 1996, pp. 303–327;
(b) F.M. Poveda, A. Sierraalta, J.L. Villaveces, F. Ruette, J. Mol. Catal. 106 (1996) 109.
[16] F. Ruette, F.M. Poveda, A. Sierraalta, J. Rivero, Surf. Sci. 349 (1996) 241.
[17] M. Sánchez, F. Ruette, J. Mol. Struct. (Theochem.) 254 (1992) 335.
[18] I. Higuerey, Comparative Study of Product Distribution of Thermal Cracking Reactions and Steam Cracking of Tia Juana Heavy Oil Residuals, Ph.D. Thesis, Universidad Central de Venezuela, 2001.
[19] F. Ruette, A. Sierralta, V. Castell, M. Laya, Carbon 31 (1993) 645.
[20] G.R. Stevenson, C.R. Wledrich, S.S. Zigler, L. Echegoyen, R. Maldonado, J. Phys. Chem. 87 (1983) 4995.
[21] R. Schogl, Alkaki metals in heterogeneous catalysis, in: H.P. Bonzel, A.M. Bradshaw, G. Ertl (Eds.), Physics and Chemistry of Alkali Metal Adsorption, Materials Science Monographs, vol. 57, Elsevier, Amsterdam, 1989, p. 347.
[22] A. Natori, T. Ohno, A. Oshiyama, J. Phys. Soc. Jpn. 54 (1985) 3042.
[23] A. Kotarba, G. Adamski, Z. Sojka, S. Witkowski, G. Djega-Mariadassou, Potassium at catalytic surfaces-stability, electronic promotion and excitation, Stud. Surf. Sci. Catal. 130 (2002) 485.
[24] I. Machín, THERMO4 (2003): Program for Thermo-chemical Calculations INTEVEP, machine@pdvsa.com.
[25] D.-H. Chen, S.-H. Wu, Chem. Mater. 12 (2000) 1354.
[26] K. Kurzak, A. Bartecki, Transit. Metal Chem. 13 (1988) 224.
[27] R.A. Ware, J. Wei, J. Catal. 93 (1985) 100.
[28] C. Adamo, F. Lelj, J. Mol. Struct. (Theochem.) 389 (1997) 83.
[29] P.A. Thiel, T.E. Madey, Surf. Sci. Rep. 7 (1987) 211.
[30] J.M. Heras, L. Viscido, Catal. Rev. -Sci. Eng. 30 (1988) 281.
[31] D.R. Lide (Ed.), Handbook of Chemistry and Physics, CRC Press, NY, 1999, pp. 10–152.
[32] J.C. de Jesús, J. Carrazza, P. Pereira, F. Zaera, Surf. Sci. 397 (1998) 34.
[33] F.A. Cotton, G. Wilkinson, Advanced Inorganic Chemistry, Interscience Publishers, New York, 1972, p. 892.